THE JOURNAL OF PHYSICAL CHEMISTRY Letters

Letter

Cite This: J. Phys. Chem. Lett. 2019, 10, 5468−5475

pubs.acs.org/JPCL

Fine Structure of Nearly Isotropic Bright Excitons in InP/ZnSe Colloidal Quantum Dots

Annalisa Brodu,[†,#] Vigneshwaran Chandrasekaran,[‡,§,#] Lorenzo Scarpelli,[∥] Jonathan Buhot,[⊥] Francesco Masia,[∥] Mariana V. Ballottin,[⊥] Marion Severijnen,[⊥] Mickaël D. Tessier,[‡,§] Dorian Dupont,[‡,§] Freddy T. Rabouw,[†] Peter C. M. Christianen,[⊥] Celso de Mello Donega,[†] Daniël Vanmaekelbergh,[*,†] Wolfgang Langbein,[*,∥] and Zeger Hens[*,‡,§]

[†]Debye Institute for Nanomaterials Science, Utrecht University, 3584 CC Utrecht, The Netherlands

[‡]Physics and Chemistry of Nanostructures, Ghent University, 9000 Ghent, Belgium

[§]Center for Nano and Biophotonics, Ghent University, 9052 Ghent, Belgium

[∥]School of Physics and Astronomy, Cardiff University, Cardiff CF24 3AA, United Kingdom

[⊥]High Field Magnet Laboratory, HFML-EMFL, Radboud University, 6525 ED Nijmegen, The Netherlands

Supporting Information

ABSTRACT: The fine structure of exciton states in colloidal quantum dots (QDs) results from the compound effect of anisotropy and electron−hole exchange. By means of single-dot photoluminescence spectroscopy, we show that the emission of photoexcited InP/ZnSe QDs originates from radiative recombination of such fine structure exciton states. Depending on the excitation power, we identify a bright exciton doublet, a trion singlet, and a biexciton doublet line that all show pronounced polarization. Fluorescence line narrowing spectra of an ensemble of InP/ZnSe QDs in magnetic fields demonstrate that the bright exciton effectively consists of three states. The Zeeman splitting of these states is well described by an isotropic exciton model, where the fine structure is dominated by electron−hole exchange and shape anisotropy leads to only a minor splitting of the $F = 1$ triplet. We argue that excitons in InP-based QDs are nearly isotropic because the particular ratio of light and heavy hole masses in InP makes the exciton fine structure insensitive to shape anisotropy.

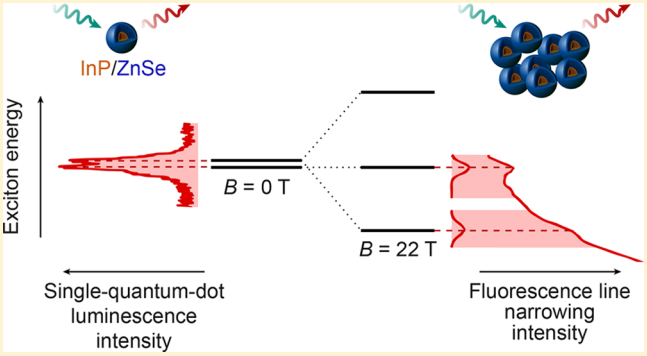

Colloidal quantum dots (QDs) are quasi-spherical semiconductor nanocrystals in which an electron−hole pair is confined in a volume with dimensions smaller than the exciton Bohr radius of the corresponding bulk material. Under such strong confinement conditions, the conduction- and valence-band edges are reduced to a set of quantized eigenstates that describe electron and hole motion. While these states can be calculated using different theoretical frameworks,[1−3] a multiband effective mass approximation has the advantage of providing analytical expressions in which semiconductors are characterized by a limited set of parameters, which are often known for the corresponding bulk material, and the QD diameter is implemented as a continuously changing variable.[2] In the case of zinc blende or wurtzite semiconductors, which include II−VI and III−V materials such as CdSe, CdTe, and InP, this approach leads to a 2-fold degenerate lowest conduction-band state and a 4-fold degenerate upper valence-band state.[2] As highlighted in panels a and b of Figure 1, these degeneracies reflect the angular momentum of the Bloch states that make up the electron states at the edge of the conduction band ($s = {}^1/_2$) and the valence band ($j = {}^3/_2$), respectively.[2] The eigenstates of electron−hole pairs or excitons are then conveniently expressed using direct products of the two different conduction-band (electron) and four different valence-band (hole) states as a basis (see Figure 1c).

Quantum dots of both wurtzite and zinc blende semiconductors have a set of fine structure eigenstates with different eigenenergies that can be described by linear combinations of the eight direct product exciton states. In the case of spherical zinc blende QDs, for example, the electron−hole exchange interaction splits the exciton levels in an optically dark low-energy quintuplet and a high-energy bright triplet that are exciton eigenstates with a total angular momentum ($F = j + s$) of 2 and 1, respectively (see Figure 1d). A further splitting of the exciton levels is obtained for QDs with an internal symmetry axis or quantization axis z, which can be the c axis for QDs with the wurtzite structure or the

Received: June 24, 2019
Accepted: August 19, 2019
Published: August 19, 2019

DOI: 10.1021/acs.jpclett.9b01824
J. Phys. Chem. Lett. 2019, 10, 5468−5475

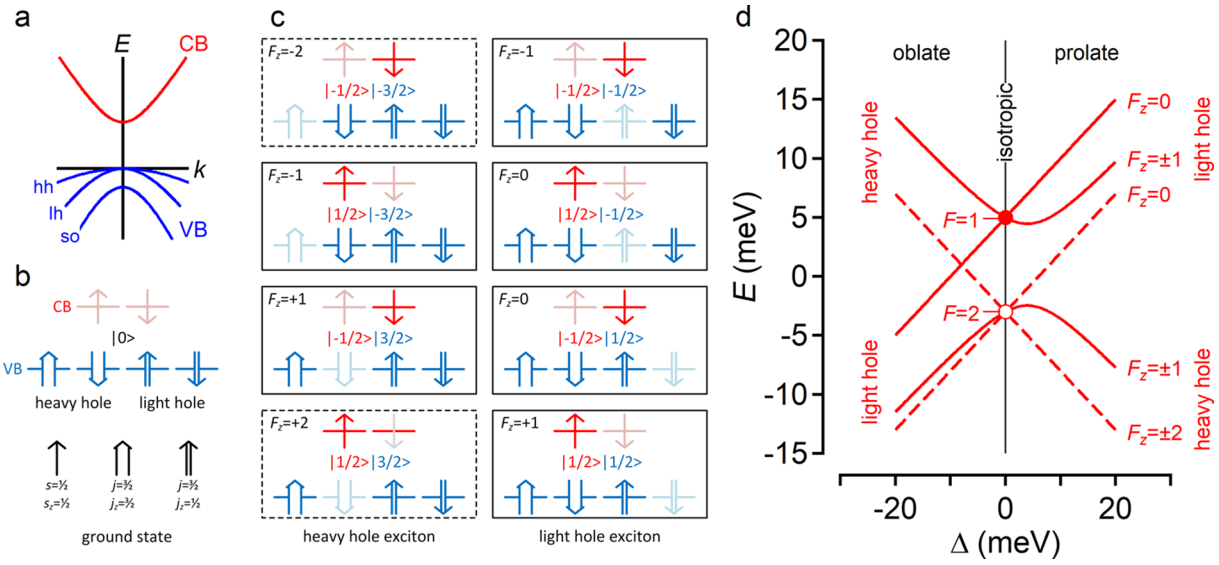

Figure 1. (a) Outline of the edges of the valence band (blue, VB) and the conduction band (red, CB) of a zinc blende semiconductor around the center of the Brillouin zone, showing the light hole (lh), heavy hole (hh), and split off (so) VB. (b) Representation of the CB and VB Bloch states at the Γ point, highlighting the degeneracy of both states in relation to their $s = {}^{1}/_{2}$ and $j = {}^{3}/_{2}$ angular momentum. Bright colors represent occupied states, and semitransparent colors empty states. (c) Overview of the eight exciton states obtained as direct products of a CB electron and a VB hole state. The states are labeled using the z-component of the total angular momentum F of the exciton. Transitions from the ground states to states boxed with a dashed line are spin-forbidden. Again, bright colors represent occupied states, and semitransparent colors empty states. (d) Exciton eigenenergies calculated as a function of the anisotropy splitting energy Δ using an exchange splitting parameter $\eta = 2$ meV. States are labeled by means of the angular momentum projection quantum number F_z along the quantization axis. Full lines represent bright states, and dashed lines dark states. Note that exchange couples the two $F_z = 0$ states to yield a bright (singlet) state and a dark (triplet) state. In the isotropic case, only the three $F = 1$ states are bright whereas the five $F = 2$ states are dark as indicated by the filled and empty circles.

rotation axis for QDs with a spheroidal shape. In such cases, five different fine structure levels are obtained, each characterized by a given projection $|F_z|$ along the quantization axis. Continuing with the example of a zinc blende QD, shape anisotropy accordingly makes the subset of heavy hole or light hole excitons the lowest-energy states, a situation typically seen with self-assembled QDs.[4] In either case, a dark exciton ground state is obtained, in combination with a 2-fold degenerate bright state at a slightly higher energy, an energy difference often described as the dark−bright splitting.

For CdSe-based colloidal QDs, multiple studies have shown that the multiband effective mass description of exciton states agrees with the experimental characteristics of these states. First, the observation that CdSe QDs exhibit longer radiative lifetimes at cryogenic temperatures was assigned to the presence of a lowest-energy dark exciton state.[5] Next, a more detailed study interpreted the different exciton features that are visible through fluorescence line narrowing (FLN) and photoluminescence excitation spectroscopy using the combined contributions from electron−hole exchange and crystal and shape anisotropy to the exciton fine structure.[6] These reports were complemented by microphotoluminescence (μ-PL) on single CdSe-based QDs, which confirmed the presence of a lowest dark state and allowed for a direct measurement of the dark−bright splitting from the respective emission lines.[7,8] More recently, this body of work was extended by the analysis of the emission of wurtzite CdSe QDs in magnetic fields, at the level of both ensembles and single QDs. These investigations highlighted the additional contribution of lateral shape anisotropy[9,10] and resulted in estimates of the electron and hole g factor.[11]

Importantly, restrictions on the use of Cd in consumer appliances have led researchers to investigate more recently InP-based QDs as a possible alternative to CdSe QDs. For InP QDs, however, the nature of the emissive state remains unclear. In line with the exciton model, time-resolved and fluorescence line narrowing photoluminescence studies confirmed the presence of a lowest-energy dark state and a higher-energy bright state, with a 5−10 meV dark−bright splitting.[12,13] Other reports, however, suggest that the photoluminescence may involve transitions between a conduction-band electron and a trapped hole.[14] In particular, a distribution of shallow hole traps may account for the persistently broad photoluminescence of InP QD ensembles and the remarkably large Stokes shift of the photoluminescence. On the other hand, studies using either photon-correlation Fourier spectroscopy in solution or μ-PL have shown that single InP/ZnSe QDs have an emission line at room temperature that is ∼50 meV wide, not unlike CdSe-based QDs.[15,16] Such discrepancies call for a more in-depth study of the InP QD fine structure, such that experimental data can be compared to predictions of the multiband effective mass model.

Here, we investigate the exciton fine structure of InP/ZnSe core/shell QDs by a combination of cryogenic single QD μ-PL and FLN spectroscopy on QD ensembles in magnetic fields. We show that the emission spectrum of single InP/ZnSe QDs exhibits three characteristic features, which we assign to the bright exciton, trion, and biexciton emission. For the example shown, the exciton and the biexciton appear as doublets split by ∼1 meV, whereas the trion emission consists of a single line for which the phonon sidebands can be well resolved. Moreover, the polarization of the trion emission closely tracks with the high-energy line in the exciton doublet. While a bright doublet could result from lateral anisotropy in the x−y plane,[9] which would split the bright $F_z = \pm 1$ level, the FLN spectra of

DOI: 10.1021/acs.jpclett.9b01824
J. Phys. Chem. Lett. 2019, 10, 5468−5475

InP/ZnSe QD ensembles show that the bright exciton consists effectively of three states that can be split by a magnetic field. This finding indicates that the bright exciton in InP/ZnSe QDs exhibits the fine structure of a nearly isotropic exciton that is split dominantly by electron−hole exchange and where the minor effect of shape anisotropy results in the bright, zero-field exciton doublet observed for single InP/ZnSe QDs.

For this study, we synthesized InP/ZnSe QDs according to the method proposed by Tessier et al.[17] In brief, we reacted indium chloride and tris(diethylaminophosphine) in oleylamine to form InP QDs, which were shelled by ZnSe by adding zinc stearate and trioctylphosphine selenium to the reaction mixture (see section S1 of the Supporting Information). As shown in Figure 2a, this resulted in a dispersion of crystalline InP/ZnSe QDs featuring an overall diameter of 10.2 ± 0.9 nm. At room temperature, we retrieved the first exciton absorption maximum at 2.09 eV (594 nm) and the exciton emission at 1.97 eV (629 nm) with a line width of 150 meV (see Figure 2b). The photoluminescence quantum yield of the dispersed InP/ZnSe QDs studied here was determined to be ∼65%.

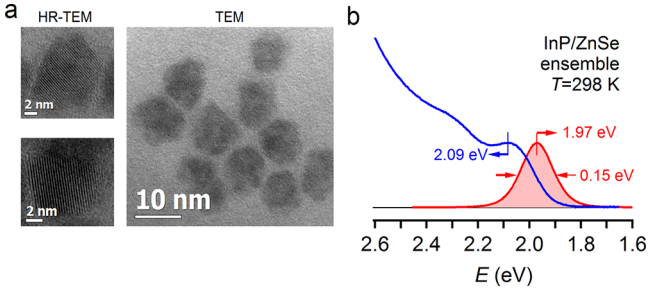

Figure 2. (a) Transmission electron microscopy (TEM) micrographs of different magnification, showing crystalline InP/ZnSe QDs with a mean diameter of 10.2 ± 0.9 nm. (b) Representation of absorption (blue) and emission (red) spectra of the ensemble of the InP/ZnSe QDs studied here.

For single-QD spectroscopy, we drop-cast a nanomolar dispersion of InP/ZnSe QDs in a 1% polystyrene/toluene solution on a quartz coverslip, which was mounted in a PL microscope (see section S2 of the Supporting Information). Using continuous-wave excitation at 473 nm while keeping the temperature set at 5 K, we observed various characteristic features in the emission spectrum of a single InP/ZnSe QD. At a relatively low excitation power, the image trace and the corresponding integrated spectrum feature a spectral doublet centered at 1.992 eV and split by an energy difference δ of 1.2 meV (see Figure 3a). Note that acoustic phonon sidebands (PSB) are visible on either side of the doublet line. With an increase in the excitation power, the time trace represented in Figure 3b features an abrupt, temporal interruption of the doublet emission that leads to a single, narrow emission line 16.5 meV to the red of the doublet line. This singlet line exhibits clear phonon sidebands at either side of the central emission line. These sidebands account for 30% of the total emission and have a maximum intensity shifted by 1.1 meV with respect to the main emission line, an energy shift that agrees with the vibrational modes of small InP nanocrystals.[18] As outlined in section S3 of the Supporting Information, we estimate a sample temperature of 9 K from the intensity ratio of the Stokes and anti-Stokes emission bands. A similar

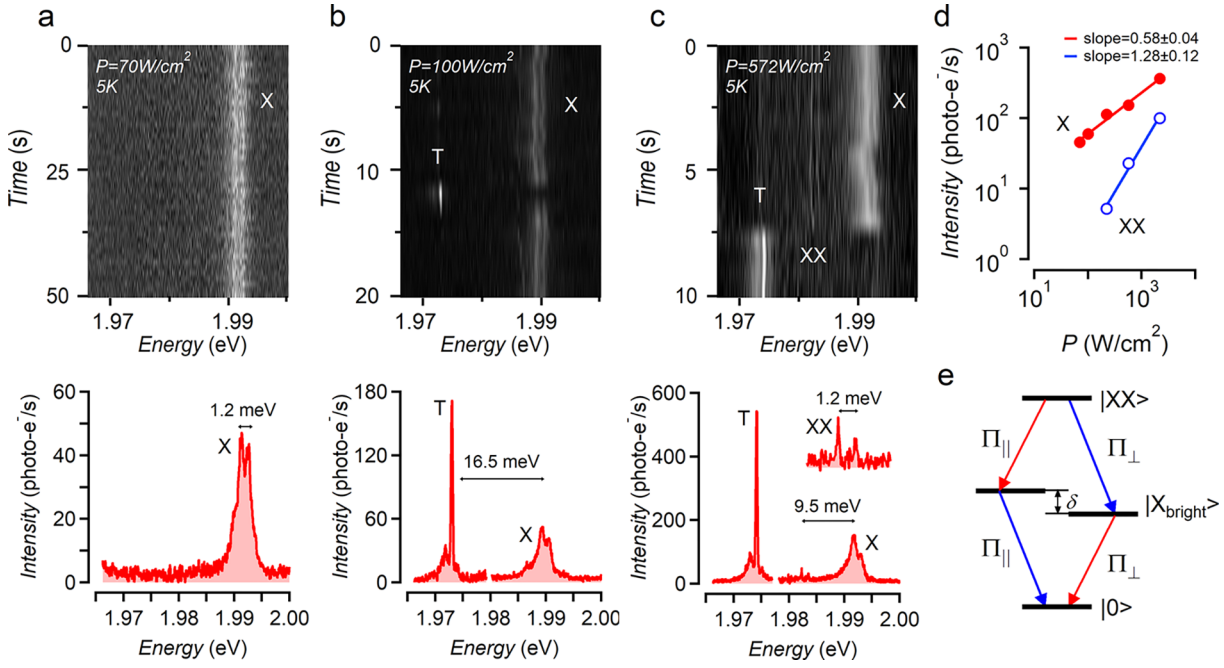

Figure 3. (a) μ-PL map (top) recorded on a single InP/ZnSe core/shell QD at cryogenic temperatures (5 K) showing the emitted intensity as a function of the photon energy and measurement time under low-power excitation. A doublet emission feature labeled X is clearly visible. Time-integrated spectrum (bottom) highlighting the spectral doublet and the energy splitting δ of 1.2 meV. The color scale in the μ-PL map has the same scale the intensity axis in the time-integrated spectrum. (b) Same as panel a under higher excitation power, showing a temporal switch between the doublet X and a singlet emission line labeled T. Both features are retained in the integrated spectrum. (c) Same as panel a under even higher excitation power, showing a similar doublet−singlet switch as in panel b and the simultaneous occurrence of a second doublet labeled XX shifted by 9.5 meV to lower energy as compared to the doublet X. (d) Integrated intensity of the X and XX doublets as a function of excitation power. (e) Scheme showing that in a biexciton−exciton ground state emission cascade, the biexciton line and the exciton line will exhibit the same splitting.

DOI: 10.1021/acs.jpclett.9b01824
J. Phys. Chem. Lett. 2019, 10, 5468−5475

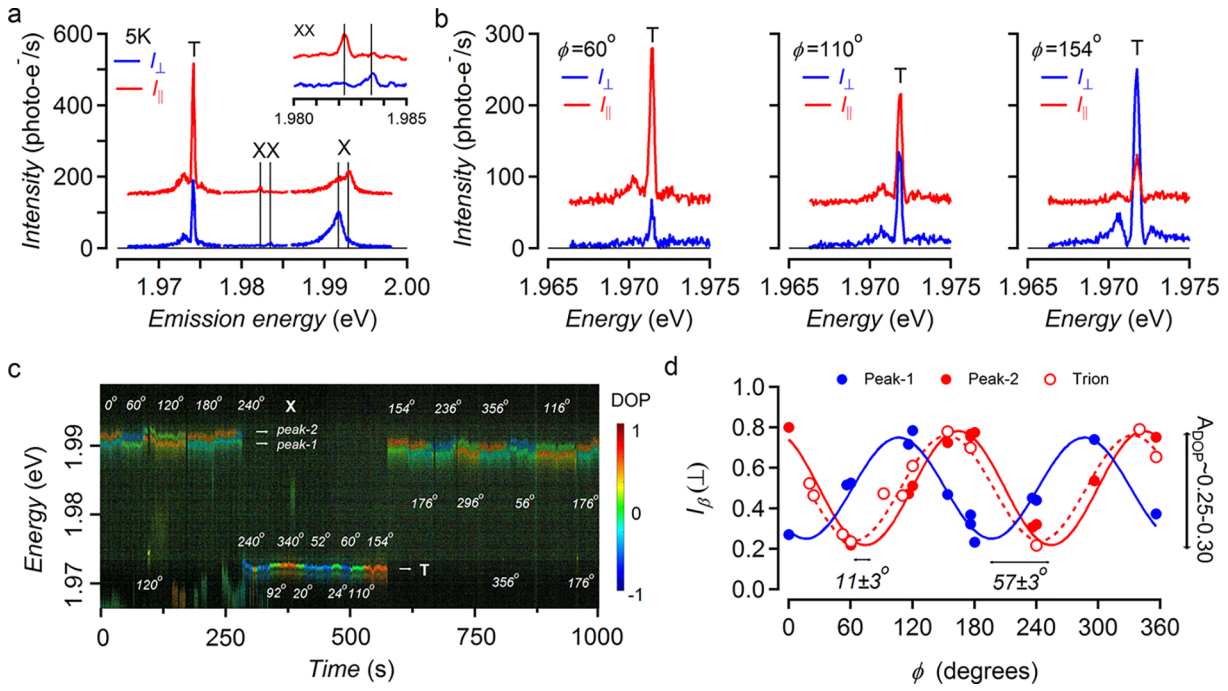

Figure 4. (a) Time-integrated emission spectrum of a single InP/ZnSe QD under excitation conditions that lead to exciton, trion, and biexciton emission as recorded in the perpendicular (blue) and parallel (red) channels. The inset shows a close-up of the biexciton doublet. For the sake of clarity, an offset of 150 photoelectrons/s was added to the parallel trace. (b) Close-ups of the trion emission for different orientations of the half-wave plate as recorded in the perpendicular and parallel channels. The polarization rotation introduced by the half-wave plate is given by $\phi = 2\theta$, where θ gives the rotation of the half-wave plate relative to a reference. (c) Color value/hue representation of the emission spectrum of a single InP/ZnSe QD as a function of time. The hue represents the degree of polarization as indicated, whereas the brightness (value) is proportional to the logarithm of the signal intensity. For brightness, the same scale is used as in the trion spectra shown in b. The indicated ϕ angles represent the temporary orientation of the half-wave plate as outlined above. (d) Relative intensity measured in the perpendicular channel as a function of the orientation of the half-wave plate for the low-energy peak of the exciton doublet (filled blue dots), the high-energy peak of the exciton doublet (filled red circles), and the trion (empty red circles). Lines represent best fits to eq 2.

switching between emission spectra characterized by a doublet line and a single line was observed in a μ-PL study of CdSe/ZnS QDs by Fernee and co-workers.[19] Assigning the doublet to exciton emission and the singlet to trion emission, these authors attributed the switching between the exciton and the trion emission to the random trapping of a band-edge carrier in a localized state.

Interestingly, at an even higher power, the switching between the doublet at around 1.992 eV and the singlet line persists, yet the doublet line now concurs with a second, low-intensity doublet. This second doublet is shifted by 9.5 meV to lower energy and features the same splitting δ of 1.2 meV (see Figure 3c). Moreover, the intensity of the higher-energy doublet as recorded using continuous-wave excitation scales sublinear with the excitation power, whereas the intensity of the additional, lower-energy doublet exhibits a supralinear excitation power scaling. As indicated in Figure 3d, fitting both power-dependent intensities to a power law yields two exponents with a ratio of 2.20 ± 0.25. Both observations support the assignment of the higher-energy doublet to the bright exciton (X) and the lower-energy doublet to the biexciton (XX). As outlined in Figure 3e, one indeed expects the transition from the biexciton to the exciton to yield an emission line that is the energetic mirror image of the bright exciton recombination. In that case, the singlet line can be assigned to a trion transition (T), not unlike previous studies of single CdSe/ZnS QDs.[19] The exciton doublet of single CdSe/ZnS QDs, on the other hand, was interpreted in terms of the exciton dark−bright splitting, where the high-energy line of the doublet corresponds to the bright exciton and the low-energy line to the dark exciton recombination. However, in the case of InP/ZnSe QDs emitting at a photon energy similar to that of the QDs studied here, the dark exciton was observed only through a broad, phonon-coupled emission feature shifted 5−15 meV to the red of the bright exciton.[13] Clearly, this observation supports the assignment of the high-energy doublet in the case of InP/ZnSe QDs to a bright exciton doublet rather than a bright−dark combination. Possibly, the combination of strong broadening and long radiative lifetimes makes the dark exciton indiscernible in the emission spectrum of single InP/ZnSe QDs. In addition, the competition between radiative recombination of the bright exciton and cooling into the dark exciton state may account for the lower than expected power scaling of the exciton and biexciton emission with increasing pump power because the presence of a dark exciton will promote nonradiative Auger recombination.

To corroborate the assignment of the three emission features to the exciton, the trion, and the biexciton, we further analyzed the polarization of the different emission lines. To do so, we successively passed the emitted light through a rotatable half-wave plate and a calcite beam displacer separating the linearly polarized components along and orthogonal to the displacement. Both parts were transmitted through the input slit of an imaging spectrometer at different positions along the slit and detected by the same CCD camera. Figure 4a shows the thus recorded spectra $I_{\parallel}$ and $I_{\perp}$ for a fixed orientation of the half-wave plate, characterized by an angle θ and thus a polarization rotation $\phi = 2\theta$, under excitation conditions where

DOI: 10.1021/acs.jpclett.9b01824
J. Phys. Chem. Lett. 2019, 10, 5468−5475

the X, T, and XX emission features are present. One sees that all the emission lines exhibit a pronounced polarization. Interestingly, the polarizations of the lines constituting the X and XX doublets are mirror images of each other. As outlined in Figure 3e, where the color coding agrees with the polarization analysis of Figure 4a, this result is expected when both lines involve the same set of split bright exciton states. The trion polarization, on the other hand, appears to coincide with that of the high-energy line of the X doublet. Focusing on the trion line, Figure 4b highlights that the intensities measured in both channels systematically change while the half-wave plate is being rotated. Starting at a ϕ of 60°, the trion emission intensity is highest in the parallel channel. Upon rotating the half-wave plate to a ϕ of 110°, one sees that the intensities in both channels become approximately equal, while the highest intensity is recorded in the perpendicular channel at a ϕ of 154°.

Using intensity $I_{\parallel}$ and $I_{\perp}$ recorded in both channels, we can define a degree of polarization (DOP) as

$$\mathrm{DOP} = \frac{I_{\parallel} - I_{\perp}}{I_{\parallel} + I_{\perp}} \tag{1}$$

Figure 4c shows an emission time trace recorded on the same InP/ZnSe QD that was analyzed in Figure 3 but represented as a value/hue plot, where the color value and hue correspond to the total emission intensity and the DOP at each time point and emission energy, respectively. The figure highlights first the systematic difference in polarization of the two lines of the bright exciton doublet. Second, because of the switching between exciton and trion emission, one can see that the polarization of the trion indeed tracks with the polarization of the high-energy line of the exciton doublet. Both observations are confirmed in Figure 4d, which represents the relative intensity in the perpendicular channel for the two exciton lines and the trion as a function of the rotation induced by the half-wave plate. The full lines in Figure 4d represent fits of the different traces to the expression

$$\frac{I_{\perp}}{I_{\parallel} + I_{\perp}} = \frac{1}{2} + A_{\mathrm{DOP}} \sin[2(\phi - \phi_0)] \tag{2}$$

As shown in Figure 4d, such fits yielded a DOP amplitude A_{DOP} in the range of 0.25−0.3 for the different transitions. Moreover, the angular difference between the two lines of the exciton doublet amounted to 57 ± 3°, whereas the polarization angle of the triplet line and the high-energy line of the exciton doublet were shifted by only 11 ± 3°.

As argued above, the observation that the PL of a single InP/ZnSe QDs randomly switches at high illumination power between a spectrum showing two doublet lines, commensurate in terms of energy splitting and polarization, and a singlet line indicates that this PL results from recombination of band-edge charge carriers rather than trapped carriers. The multiband effective mass model of the band-edge exciton fine structure provides two possible interpretations of a bright doublet in QDs with a zinc blende crystal structure. First, as shown in Figure 1d, pronounced shape anisotropy brings either the light hole or heavy hole exciton states down in energy, which are both 4-fold degenerate states that are further split by exchange interaction to give exciton states with a fixed component of the angular moment F_z along the quantization axis z. This situation is detailed in Figure 5a for the case in which the light hole is lowest in energy. This yields a fine structure in which a bright

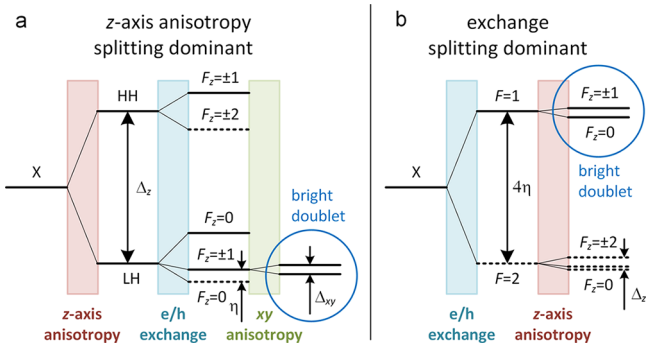

Figure 5. (a) Sequence of splitting of the exciton states when z axis anisotropy dominates, for a case in which the light hole exciton is lowered in energy. In that case, a bright exciton doublet can result from additional anisotropy in the x−y plane. (b) Sequence of splitting of the exciton states when exchange dominates. In that case, a bright exciton doublet can result from a minor z axis anisotropy. In both figures, η is the exchange parameter and Δ the anisotropy energy for the ground state exciton,[20] whereas full lines represent bright exciton states and dashed lines dark exciton states.

$F_z = \pm 1$ exciton doublet is separated from the $F_z = 0$ dark ground state by the exchange interaction and from the higher-energy bright $F_z = 0$ exciton singlet by thrice the exchange interaction.[20] Additional anisotropy in the x−y plane will split this isolated $F_z = \pm 1$ exciton into two components,[9,10] emitting light linearly polarized along the x and y axes.[21] When the heavy hole states are lowest in energy, a similar situation arises in which the lowest-energy bright state is an $F_z = \pm 1$ exciton that will be split by lateral anisotropy. Second, when the exchange interaction dominates, shape anisotropy will merely split the upper bright triplet into two components, a first with angular momentum $F_z = 0$ and a second with angular momentum $F_z = \pm 1$ (see Figure 5b). Such excitons will emit light linearly polarized along the z axis and light circularly polarized within the x−y plane, respectively. Finally, while shape anisotropy makes the low-energy $F_z = \pm 1$ exciton bright through coupling with the high-energy $F_z = \pm 1$ exciton, this effect remains negligible for small deviations from the isotropic case. Hence, the lower-energy $F_z = \pm 1$ exciton is represented by a dashed line in Figure 5b.

To determine the overall degeneracy of the bright exciton, 2-fold with a minor splitting due to anisotropy in the x−y plane or 3-fold with a minor splitting due to anisotropy along the z axis (see Figure 5), we analyzed the emission of an ensemble of InP/ZnSe QDs by FLN spectroscopy in a magnetic field. For this study, a sample with a peak emission at 2.12 eV at 4 K was used (see section S4 of the Supporting Information), which we pumped resonantly at 2.06 eV using a monochromatic laser source. While not exactly identical, these experimental settings are in good correspondence with the single InP/ZnSe QDs discussed above. As outlined in section S4 of the Supporting Information, FLN spectra were acquired in Faraday configuration with the excitation light parallel to the direction of the magnetic field. The excitation light had a σ^+ circular polarization, which dominantly excites the $F_z = 1$ state in the given configuration, while we detected emitted light with σ^- polarization.

Figure 6a shows the FLN spectra acquired in the absence of a magnetic field using the excitation conditions described above. Note that we use the energy difference $\Delta E = \hbar\omega_{\mathrm{exc}} - \hbar\omega_{\mathrm{em}}$ between the excitation and emitted photons as the

DOI: 10.1021/acs.jpclett.9b01824
J. Phys. Chem. Lett. 2019, 10, 5468−5475

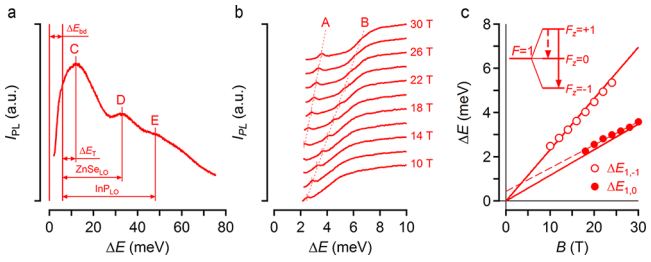

Figure 6. (a) Fluorescence line narrowing (FLN) spectrum of an ensemble of InP/ZnSe QDs excited using 2.06 eV, σ^+ polarized light. The energy difference ΔE measures the energy loss of the emitted phonons relative to 2.06 eV. Using the energy of the ZnSe and InP optical phonon as a yardstick, the indicated features are assigned to the acoustic phonon replica of dark state emission (C), the ZnSe LO phonon replica of dark state emission (D), and the InP LO phonon replica of dark state emission (E). From this analysis, we obtain a bright−dark splitting energy ΔE_{bd} of 6 meV. (b) FLN spectra of the same InP/ZnSe QD ensemble in different magnetic fields as indicated. The dashed line highlights the two additional emission features, labeled A and B, that appear in the spectra, whereas the short vertical lines indicate the estimated shift of each feature relative to the excited level. (c) Energy shift of features A and B with respect to the photoexcited $F_z = 1$ state. The full lines represent the result of a global fit to the expression of the isotropic exciton model, using g_h as the only adjustable parameter ($\Delta E_{bd} = 6$ meV, $g_e = 1.6$, and $g_h = -1.925$). The thin dashed line is an extrapolation of the experimental data.

horizontal axis. The three broad features labeled C−E in the FLN spectrum were assigned previously to the phonon-activated dark exciton emission (C) and replicas of this transition involving the additional emission of ZnSe (D) and InP LO phonons (E).[13] Using the latter two as a yardstick, we estimate the bright−dark splitting in these InP/ZnSe QDs at a ΔE_{bd} of 6 meV (see Figure 6a). In Figure 6b, we show the low-energy part of various FLN spectra obtained on the same InP/ZnSe QD ensemble with an increase in the magnetic field from 10 to 30 T. Interestingly, we observe two additional features that shift to lower energy relative to the $F_z = 1$ state with an increase in the magnetic field. A first, labeled as A, can be discerned for fields of ≥18 T and shifts from $\Delta E = 2.25$ to 3.58 meV at 30 T (see section S4 of the Supporting Information). A second, labeled B, appears first at fields of 10 T. This feature shifts more strongly with an increase in field strength, from 2.48 meV at 10 T to 5.35 meV at 24 T. For the largest fields, the feature is reduced to a mere shoulder on top of the rising side of the phonon-assisted dark exciton emission, making unreliable any determination of the energy shift. For both features, Figure 6c summarizes the energy shift as a function of the magnetic field, where we label the energies at which features A and B are retrieved as $\Delta E_{1,0}$ and $\Delta E_{1,-1}$, respectively.

The observation of two emission features, shifting to lower energy with respect to the excited $F_z = 1$ bright state, shows that in the absence of a magnetic field, the excited bright exciton consists of three different, nearly degenerate states. This result strongly contrasts with similar measurements of wurtzite CdSe QDs, which showed a bright exciton doublet.[9] We thus conclude that the spectral doublet of the single InP/ZnSe QD analyzed in Figure 3 should be seen as a nearly isotropic exciton subject to minor splitting in a singlet and a doublet state due to anisotropy along quantization axis.

For an isotropic exciton, the energy splitting $\Delta E_{1,0} = E_1 - E_0$ and $\Delta E_{1,-1} = E_1 - E_{-1}$ among the three bright exciton states depends on the applied magnetic field according to (see section S5 of the Supporting Information):

$$\Delta E_{1,0} = -g_h \mu_B B + \sqrt{3\eta^2 + \left(\eta - \frac{g_e + g_h}{2}\mu_B B\right)^2} - \sqrt{4\eta^2 + \left(\frac{g_e + g_h}{2}\mu_B B\right)^2} \quad (3)$$

$$\Delta E_{1,-1} = -2g_h \mu_B B + \sqrt{3\eta^2 + \left(\eta - \frac{g_e + g_h}{2}\mu_B B\right)^2} - \sqrt{3\eta^2 + \left(\eta + \frac{g_e + g_h}{2}\mu_B B\right)^2} \quad (4)$$

where the exchange parameter η corresponds to a quarter of the bright−dark splitting between the high-energy $F = 1$ and low-energy $F = 2$ states (see Figure 5b),[20] g_e and g_h are the gyromagnetic ratios of the electron and the hole, respectively, and μ_B is the Bohr magneton. In writing eqs 3 and 4, we took as a convention that for positive values of g_h, the energy of hole states with the angular momentum parallel to the magnetic field is decreased whereas for positive values of g_e, the energy of electron states with angular momentum antiparallel to the field is decreased.[22] Unless $|g_h| \ll |g_e|$, the first term in eqs 3 and 4 will be dominant, and a negative g_h is needed to make the $F_z = 1$ state the high-energy state. As shown in section S6 of the Supporting Information, keeping η fixed at 1.5 meV yields satisfactory global fits of the experimental data to eqs 3 and 4, yet such fits do not allow for an accurate determination of g_e and g_h separately. We therefore sought best fits while keeping g_e fixed at values in the range of 1.0−2.0, which encompasses the electron g factor for bulk InP and values reported for self-assembled InP-based QDs.[23] Figure 6c represents such a fit, where we took a g_e of 1.6, a value previously reported for InP/(In,Ga)P self-assembled QDs,[23] and obtained a best fit for a g_h of -1.93 ± 0.03. As outlined in section S6 of the Supporting Information, sweeping g_e from 1.0 to 2.0 has only a minor impact on the best fit for g_h, which we accordingly estimated to be -1.9 ± 0.1. Interestingly, this number is in reasonable agreement with the estimate for g_h of −1.49 we calculated using the expression proposed by Efros et al. (see section S7 of the Supporting Information).[20] Similarly negative values have been predicted for multiple spherical II−VI QDs,[22] and a g_h value of −0.73 was derived from Faraday rotation measurements in the case of wurtzite CdSe QDs.[24]

Upon close examination of Figure 6c, it appears that the isotropic exciton model slightly underestimates the energy splitting $\Delta E_{1,0}$ between the $F_z = 1$ and $F_z = 0$ states. At least, a linear fit to the experimental data yields a line lying systematically higher than the global fit. This could reflect a minor splitting of the three $F = 1$ exciton states at zero field, in line with the bright exciton doublet measured on a single InP/ZnSe QD. Given the slightly larger than expected $\Delta E_{1,0}$ splitting, the low-energy line of the doublet would then correspond to the $F_z = 0$ state and the high-energy line to the $F_z = \pm 1$ states. Such an assignment can explain the different polarization of both lines because the $F_z = 0$ state emits linearly polarized light with an electric field along the quantization axis, whereas the $F_z = \pm 1$ states emit circularly polarized light with the electric field in the x−y plane. Note that the particular viewing angle on a given QD can make that circularly polarized

DOI: 10.1021/acs.jpclett.9b01824
J. Phys. Chem. Lett. 2019, 10, 5468−5475

emission appear as partially linearly polarized in the detection system used and that the phase difference between both emission lines differs from 90°. Interestingly, in the case of isotropic QDs, theoretical work indicates that the negative trion ground state emits circularly polarized light because the hole occupies either the $j_z = {}^3/_2$ or the $j_z = -{}^3/_2$ heavy hole level.[25] The positive trion, on the other hand, has a mixed ground state that leads to a set of recombination pathways emitting either circular or linear polarized light.[25] Hence, the correspondence between the polarization of the high-energy exciton doublet line and the trion singlet line might point toward emission from the negative trion. Such a conclusion needs, however, the confirmation from a more in-depth study of these emission lines, for example, to account for artifacts induced by the viewing angle on a given QD.

Via single-QD PL and FLN spectroscopy, we have gained evidence that radiative exciton recombination contributes to the photoluminescence of InP/ZnSe QDs. While this finding does not rule out trap-related emission pathways,[14] it does highlight the fact that trap-related emission is not the dominant recombination process in these QDs. In more general terms, the observation that excitons in InP/ZnSe QDs are nearly isotropic is far from trivial. In the case of CdSe QDs, for example, little difference was observed between the exciton fine structure of nanocrystals with a wurtzite and a zinc blende crystal structure.[26] Whereas wurtzite CdSe is intrinsically anisotropic, it was argued that relatively small deviations from a spherical shape can account for the similar anisotropy of the exciton in zinc blende CdSe QDs. Similary, an exciton model including exchange and shape anisotropy was used to describe the emission features of single zinc blende CdTe QDs.[27] Both examples suggest that deviations from an isotropic, spherical shape are to be expected in the case of colloidal QDs, and it is not clear why InP QDs should be an exception here. According to the exciton description developed by Efros, however, the impact of deviations from a spherical shape on the exciton fine structure depends on the light hole to heavy hole mass ratio ($\beta = m_{lh}/m_{hh}$). Interestingly, the model predicts that the fine structure of the exciton will be insensitive to shape anisotropy when $\beta = 0.14$, which means that under such conditions also prolate or oblate ellipsoids will host isotropic excitons.[20] In the case of InP, β depends on the direction in reciprocal space, yet an average of β over the (100), (110), and (111) directions yields a value of 0.149.[28] In contrast, for wz-CdSe, the hole mass ratio amounts to 0.28,[6] a value at which the impact of shape anisotropy on the fine structure is approximately maximal.[20] Possibly, having an average hole mass ratio close to the critical value of 0.14 is what makes InP-based QDs host nearly isotropic excitons.

In summary, we have investigated the emission of InP/ZnSe QDs using a combination of cryogenic microphotoluminescence spectroscopy of single InP/ZnSe QDs and fluorescence line narrowing spectroscopy on an ensemble of InP/ZnSe QDs. We show that the emission is related to exciton recombination, where the spectrum of a single InP/ZnSe features a bright exciton doublet, a trion singlet, and a biexciton doublet. FLN spectra recorded versus magnetic field strength demonstrate that this bright exciton doublet reflects a minor deviation from the 3-fold degenerate, isotropic bright exciton expected in spherical QDs with a zinc blende structure. We assign the observation of nearly isotropic excitons in InP/ZnSe QDs to the InP average hole mass ratio β of 0.149. In contrast with CdSe ($\beta = 0.28$), this number is close to the value of 0.14 at which the exciton fine structure is insensitive to shape anisotropy.[20] From a fundamental perspective, isotropic excitons are highly interesting model systems for experimental studies and theory development. Different from anisotropic excitons, isotropic excitons have a fine structure solely determined by the exchange splitting. This makes the bright−dark splitting of isotropic excitons ideally suited for comparison of the predicted size dependence of the exchange interaction with experimental data. In addition, the interaction between an isotropic exciton and an external field is independent of the QD orientation. As exemplified by the FLN study shown here, this indicates that ensemble measurements in external fields are not compounded by orientation averaging, such that material characteristics can be determined in a direct manner from the analysis of ensembles. We therefore believe that the observation of nearly isotropic excitons in InP-based QDs opens a new direction for investigating the exciton fine structure in nanoscale semiconductors.

■ ASSOCIATED CONTENT

Supporting Information

The Supporting Information is available free of charge on the ACS Publications website at DOI: 10.1021/acs.jpclett.9b01824.

Background on the synthesis protocol (section S1), the setup for micro-PL analysis (section S2), analysis of the phonon temperature (section S3), fluoresecence line narrowing spectroscopy (section S4), splitting of the isotropic exciton in a magnetic field (section S5), fits of the FLN data to the isotropic exciton model (section S6), and an estimate of the hole g factor (section S7) (PDF)

■ AUTHOR INFORMATION

Corresponding Authors

*E-mail: d.vanmaekelbergh@uu.nl.
*E-mail: langbeinww@cardiff.ac.uk.
*E-mail: zeger.hens@ugent.be.

ORCID

Mickaël D. Tessier: 0000-0003-0950-091X
Freddy T. Rabouw: 0000-0002-4775-0859
Celso de Mello Donega: 0000-0002-4403-3627
Daniël Vanmaekelbergh: 0000-0002-3535-8366
Wolfgang Langbein: 0000-0001-9786-1023
Zeger Hens: 0000-0002-7041-3375

Author Contributions

#A.B. and V.C. contributed equally to this work.

Notes

The authors declare no competing financial interest.

■ ACKNOWLEDGMENTS

Z.H., D.V., and W.L. acknowledge support from the European Commission via the Marie-Sklodowska Curie action Phonsi (H2020-MSCA-ITN-642656). Z.H. acknowledges support by SIM-Flanders (SBO-QDOCCO), FWO-Vlaanderen (Research Project 17006602), and Ghent University (GOA 01G01019). F.T.R. is supported by NWO Veni Grant 722.017.002 and by The Netherlands Center for Multiscale Catalytic Energy Conversion (MCEC), an NWO Gravitation program funded by the Ministry of Education, Culture and Science of the

DOI: 10.1021/acs.jpclett.9b01824
J. Phys. Chem. Lett. 2019, 10, 5468−5475

government of The Netherlands. F.M. acknowledges the Ser Cymru II programme (Case ID 80762-CU-148) which is partly funded by Cardiff University and the European Regional Development Fund through the Welsh Government. This work was supported by HFML-RU/FOM, member of the European Magnetic Field Laboratory (EMFL).

REFERENCES

(1) Franceschetti, A.; Zunger, A. Direct Pseudopotential Calculation of Exciton Coulomb and Exchange Energies in Semiconductor Quantum Dots. *Phys. Rev. Lett.* **1997**, *78*, 915−918.
(2) Efros, A.; Rosen, M. The Electronic Structure of Semiconductor Nanocrystals. *Annu. Rev. Mater. Sci.* **2000**, *30*, 475−521.
(3) Niquet, Y.; Delerue, C.; Allan, G.; Lannoo, M. Method for Tight-Binding Parametrization: Application to Silicon Nanostructures. *Phys. Rev. B: Condens. Matter Mater. Phys.* **2000**, *62*, 5109−5116.
(4) Huo, Y. H.; Witek, B. J.; Kumar, S.; Cardenas, J. R.; Zhang, J. X.; Akopian, N.; Singh, R.; Zallo, E.; Grifone, R.; Kriegner, D.; Trotta, R.; Ding, F.; Stangl, J.; Zwiller, V.; Bester, G.; Rastelli, A.; Schmidt, O. G. A Light-Hole Exciton in a Quantum Dot. *Nat. Phys.* **2014**, *10*, 46−51.
(5) Nirmal, M.; Norris, D. J.; Kuno, M.; Bawendi, M. G.; Efros, A. L.; Rosen, M. Observation of the "Dark Exciton" in CdSe Quantum Dots. *Phys. Rev. Lett.* **1995**, *75*, 3728−3731.
(6) Norris, D. J.; Efros, A. L.; Rosen, M.; Bawendi, M. G. Size Dependence of Exciton Fine Structure in CdSe Quantum Dots. *Phys. Rev. B: Condens. Matter Mater. Phys.* **1996**, *53*, 16347−16354.
(7) Labeau, O.; Tamarat, P.; Lounis, B. Temperature Dependence of the Luminescence Lifetime of Single CdSe/ZnS Quantum Dots. *Phys. Rev. Lett.* **2003**, *90*, 257404.
(8) Biadala, L.; Louyer, Y.; Tamarat, P.; Lounis, B. Direct Observation of the Two Lowest Exciton Zero-Phonon Lines in Single CdSe/ZnS Nanocrystals. *Phys. Rev. Lett.* **2009**, *103*, No. 037404.
(9) Furis, M.; Htoon, H.; Petruska, M. A.; Klimov, V. I.; Barrick, T.; Crooker, S. A. BrightExciton Fine Structure and Anisotropic Exchange in CdSe Nanocrystal Quantum Dots. *Phys. Rev. B: Condens. Matter Mater. Phys.* **2006**, *73*, 241313.
(10) Htoon, H.; Furis, M.; Crooker, S. A.; Jeong, S.; Klimov, V. I. Linearly Polarized 'Fine Structure' of the Bright Exciton State in Individual CdSe Nanocrystal Quantum Dots. *Phys. Rev. B: Condens. Matter Mater. Phys.* **2008**, *77*, No. 035328.
(11) Granados del Aguila, A.; Pettinari, G.; Groeneveld, E.; de Mello Donega, C.; Vanmaekelbergh, D.; Maan, J. C.; Christianen, P. C. M. Optical Spectroscopy of Dark and Bright Excitons in CdSe Nanocrystals in High Magnetic Fields. *J. Phys. Chem. C* **2017**, *121*, 23693−23704.
(12) Biadala, L.; Siebers, B.; Beyazit, Y.; Tessier, M. D.; Dupont, D.; Hens, Z.; Yakovlev, D. R.; Bayer, M. Band-Edge Exciton Fine Structure and Recombination Dynamics in InP/ZnS Colloidal Nanocrystals. *ACS Nano* **2016**, *10*, 3356−3364.
(13) Brodu, A.; Ballottin, M. V.; Buhot, J.; van Harten, E. J.; Dupont, D.; La Porta, A.; Prins, P. T.; Tessier, M. D.; Versteegh, M. A. M.; Zwiller, V.; Bals, S.; Hens, Z.; Rabouw, F. T.; Christianen, P. C. M.; de Mello Donega, C.; Vanmaekelbergh, D. Exciton Fine Structure and Lattice Dynamics in InP/ZnSe Core/Shell Quantum Dots. *ACS Photonics* **2018**, *5*, 3353−3362.
(14) Janke, E. M.; Williams, N. E.; She, C.; Zherebetskyy, D.; Hudson, M. H.; Wang, L.; Gosztola, D. J.; Schaller, R. D.; Lee, B.; Sun, C.; Engel, G. S.; Talapin, D. V. Origin of Broad Emission Spectra in InP Quantum Dots: Contributions from Structural and Electronic Disorder. *J. Am. Chem. Soc.* **2018**, *140*, 15791−15803.
(15) Cui, J.; Bayler, A. P.; Marshall, L. F.; Chen, O.; Harris, D. K.; Wanger, D. D.; Brokmann, X.; Bawendi, M. G. Direct Probe of Spectral Inhomogeneity Reveals Synthetic Tunability of Single-Nanocrystal Spectral Linewidths. *Nat. Chem.* **2013**, *5*, 602−606.
(16) Chandrasekaran, V.; Tessier, M. D.; Dupont, D.; Geiregat, P.; Hens, Z.; Brainis, E. Nearly Blinking-Free, High-Purity Single-Photon Emission by Colloidal InP/ZnSe Quantum Dots. *Nano Lett.* **2017**, *17*, 6104−6109.
(17) Tessier, M. D.; Dupont, D.; De Nolf, K.; De Roo, J.; Hens, Z. Economic and Size-Tunable Synthesis of InP/ZnE (E = S, Se) Colloidal Quantum Dots. *Chem. Mater.* **2015**, *27*, 4893−4898.
(18) Talati, M.; Jha, P. K. Acoustic Phonons in Semiconductor Nanocrystals. *Comput. Mater. Sci.* **2006**, *37*, 58−63.
(19) Fernée, M. J.; Littleton, B. N.; Rubinsztein-Dunlop, H. Detection of Bright Trion States Using the Fine Structure Emission of Single CdSe/ZnS Colloidal Quantum Dots. *ACS Nano* **2009**, *3*, 3762−3768.
(20) Efros, A. L.; Rosen, M.; Kuno, M.; Nirmal, M.; Norris, D. J.; Bawendi, M. Band-Edge Exciton in Quantum Dots of Semiconductors with a Degenerate Valence Band: Dark and Bright Exciton States. *Phys. Rev. B: Condens. Matter Mater. Phys.* **1996**, *54*, 4843−4856.
(21) Barak, Y.; Meir, I.; Shapiro, A.; Jang, Y.; Lifshitz, E. Fundamental Properties in Colloidal Quantum Dots. *Adv. Mater.* **2018**, *30*, 1801442.
(22) Shornikova, E. V.; Biadala, L.; Yakovlev, D. R.; Feng, D.; Sapega, V. F.; Flipo, N.; Golovatenko, A. A.; Semina, M. A.; Rodina, A. V.; Mitioglu, A. A.; Ballottin, M. V.; Christianen, P. C. M.; Kusrayev, Y. G.; Nasilowski, M.; Dubertret, B.; Bayer, M. Electron and Hole g-Factors and Spin Dynamics of Negatively Charged Excitons in CdSe/CdS Colloidal Nanoplatelets with Thick Shells. *Nano Lett.* **2018**, *18*, 373−380.
(23) Syperek, M.; Yakovlev, D. R.; Yugova, I. A.; Misiewicz, J.; Jetter, M.; Schulz, M.; Michler, P.; Bayer, M. Electron and Hole Spins in InP/(Ga,In)P Self-Assembled Quantum Dots. *Phys. Rev. B: Condens. Matter Mater. Phys.* **2012**, *86*, 125320.
(24) Gupta, J. A.; Awschalom, D. D.; Efros, A. L.; Rodina, A. V. Spin Dynamics in Semiconductor Nanocrystals. *Phys. Rev. B: Condens. Matter Mater. Phys.* **2002**, *66*, 125307.
(25) Shabaev, A.; Rodina, A. V.; Efros, A. L. Fine Structure of the Band-Edge Excitons and Trions in CdSe/CdS Core/Shell Nanocrystals. *Phys. Rev. B: Condens. Matter Mater. Phys.* **2012**, *86*, 205311.
(26) Moreels, I.; Raino, G.; Gomes, R.; Hens, Z.; Stoferle, T.; Mahrt, R. F. Band-Edge Exciton Fine Structure of Small, Nearly Spherical Colloidal CdSe/ZnS Quantum Dots. *ACS Nano* **2011**, *5*, 8033−8039.
(27) Tilchin, J.; Rabouw, F. T.; Isarov, M.; Vaxenburg, R.; Van Dijk-Moes, R. J. A.; Lifshitz, E.; Vanmaekelbergh, D. Quantum Confinement Regimes in CdTe Nanocrystals Probed by Single Dot Spectroscopy: From Strong Confinement to the Bulk Limit. *ACS Nano* **2015**, *9*, 7840−7845.
(28) Kim, Y.-S.; Hummer, K.; Kresse, G. Accurate Band Structures and Effective Masses for InP, InAs, and InSb Using Hybrid Functionals. *Phys. Rev. B: Condens. Matter Mater. Phys.* **2009**, *80*, No. 035203.

DOI: 10.1021/acs.jpclett.9b01824
J. Phys. Chem. Lett. 2019, 10, 5468−5475